Ceramics International 46 (2020) 3949–3959

Contents lists available at ScienceDirect

Ceramics International

journal homepage: www.elsevier.com/locate/ceramint

Antibacterial properties of laser surface-textured TiO_2/ZnO ceramic coatings

Yusliza Yusuf[a,b,*], Mariyam Jameelah Ghazali[a,**], Yuichi Otsuka[c], Kiyoshi Ohnuma[d], Sarita Morakul[e], Susumu Nakamura[f], Mohd Fadzli Abdollah[g]

[a] Centre for Materials Engineering and Smart Manufacturing, Faculty of Engineering and Built Environment, Universiti Kebangsaan Malaysia,UKM, Bangi, 43600, Selangor, Malaysia
[b] Fakulti Teknologi Kejuruteraan Mekanikal dan Pembuatan, Universiti Teknikal Malaysia Melaka, Hang Tuah Jaya, Durian Tunggal, Melaka, 76100, Malaysia
[c] Department of System Safety, Nagaoka University of Technology, 1603-1 Kamitomioka, Nagaoka, Niigata, 940-2188, Japan
[d] Department of Bioengineering, Nagaoka University of Technology, 1603-1 Kamitomioka, Nagaoka, Niigata, 940-2188, Japan
[e] Graduate School of Material Science, Nagaoka University of Technology, 1603-1 Kamitomioka, Nagaoka, Niigata, 940-2188, Japan
[f] Department of Electrical and Electronic Systems Engineering, National Institute of Technology, Nagaoka College, 888 Nishikatakai, Nagaoka, Niigata, 940-8523, Japan
[g] Fakulti Kejuruteraan Mekanikal, Universiti Teknikal Malaysia Melaka, Hang Tuah Jaya, Durian Tunggal, Melaka, 76100, Malaysia

ARTICLE INFO

Keywords:
Surfaces (B)
TiO_2 (D)
ZnO (D)
Functional applications (E)

ABSTRACT

Bacterial attachment on surfaces cause fouling, which reduces the hygiene status and effectiveness of equipment. Preventing bacterial attachment on surfaces through surface modification is a potential solution to fouling and has thus become a key research area. In this study, the effect of different ZnO contents (wt%) and picosecond laser surface texturing on the antibacterial properties of TiO_2/ZnO ceramic coatings were investigated. The attachment and viability of *Escherichia coli (E. coli)* bacteria on laser surface-textured and non-textured TiO_2/ZnO ceramic coatings were explored. Bacterial growth in an immersion suspension was evaluated using the optical density method. The number of colony-forming units on laser surface-textured TiO_2/ZnO coatings was found to be lower than that on non-textured coatings, which indicates that laser surface-textured coatings demonstrate strong antibacterial properties. Furthermore, the number of viable *E. coli* bacteria on laser surface-textured TiO_2/ZnO coatings was observed to be lower than that on non-textured coatings. This finding also demonstrates that laser surface texturing enhances the antibacterial properties of TiO_2/ZnO coatings. Overall, laser surface texturing increased the surface areas of the coatings and improved the effectiveness of ZnO as an antibacterial agent. These results prove that laser surface texturing is a successful method for fabricating antibacterial surfaces.

1. Introduction

Surface fouling can be attributed to the deposition and accumulation of undesirable substances on functional surfaces, and it affects the functionality of the surfaces. Biofouling materials may be composed of living organisms, such as algae and mussels, and materials involved in common industrial fouling may be composed of organic and inorganic matter [1–3]. Because surface fouling can negatively affect the operating productivity of equipment by reducing transportation effectiveness, it can cause various economic and contamination issues in numerous industries, including the oil, gas and food industries, which result in high maintenance costs. In general, fouling begins with the initial attachment and subsequent multiplication of bacteria on substrate surfaces [4]. The initial bacterial surface attachment is governed by physical interactions between the bacteria and the substrate surfaces, and biological processes occur over long time scales [5]. Several factors, including bacterial properties, substrate surface characteristics and environmental conditions, influence this attachment process [5]. Bacterial adhesion is related to surface topography, and the modification of surface properties, such as topography, chemistry and physicochemistry, may enhance or reduce bacterial attachment. Numerous studies have been performed to determine the effect of surface topographical properties on bacterial attachment [6–8], and some studies have shown that bacterial attachment is strongly affected by surface roughness [7,9] and surface wettability [10,11]. Meanwhile, several studies have focused on loading antibacterial agents onto surfaces to avoid the possible adverse effects caused by bacterial attachment [12,13]. Several metallic oxides, such as TiO_2, ZnO, CaO, SiO_2 and

* Corresponding author. Centre for Materials Engineering and Smart Manufacturing, Faculty of Engineering and Built Environment, Universiti Kebangsaan Malaysia,UKM, Bangi, 43600, Selangor, Malaysia.
** Corresponding author.
E-mail addresses: yusliza@utem.edu.my (Y. Yusuf), mariyam@ukm.edu.my (M.J. Ghazali).

https://doi.org/10.1016/j.ceramint.2019.10.124
Received 8 May 2019; Received in revised form 14 October 2019; Accepted 14 October 2019
Available online 15 October 2019

Table 1
Mixing ratios of the powders used as feedstock in the plasma spraying process.

Sample label	Mixing ratios of powders	
	TiO_2 (g)	ZnO (g)
A1	100	0
A2	90	10
A3	70	30

Table 2
Process parameters for atmospheric plasma spraying.

Parameter	Value
Arc current (A)	600
Primary gas: argon (psi)	80
Secondary gas: helium (psi)	40
Carrier gas: argon (psi)	30
Powder feed rate (rpm)	4
Spraying distance (mm)	80
Robot speed (mm/s)	250
Number of pre-heat cycles	2

Al_2O_3, have been widely used as antibacterial agents because of their stability and durability under ultraviolet (UV) light irradiation. ZnO is especially promising because of its resistance to bacteria in the absence or presence of UV light. Furthermore, ZnO does not modify the pH or concentration of the surrounding medium [14].

The present study introduced laser surface textured TiO_2/ZnO mix of the two oxides coatings on the basis of the antibacterial effect of TiO_2 and ZnO against a broad spectrum of bacterial species [15]. Laser surface texturing involves creating different patterns on substrates and has been proven effective in improving surface features [16–19], and the use of laser surface texturing or laser surface modification to produce surfaces with different applications has been extensively studied [16,20]. This method is favourable because (i) it enables the surface roughness to be controlled from the nano-to microscale without drastically changing surface composition, (ii) it is a single-step process under ambient conditions and (iii) it is applicable with a wide range of material types [21,22]. Moreover, modifying the surface morphology can enhance or reduce the antibacterial properties of materials [12]. Many studies have been conducted to determine the effect of surface properties on bacterial attachment and retention [23–26]. Some studies have reported that surface modification, such as changing the topographical properties of the surface, affects the initial bacterial attachment on surfaces [5,27,28]. Additional factors, including inherent bacterial properties, material surface characteristics and environmental conditions under which growth occurs, further influence bacterial attachment [5,29]. Despite the development of numerous micro- and nanotopographically engineered antibacterial surfaces, a general consensus on the interaction between bacterial attachment, surface modification and material surface characteristics has yet to be reached.

This study aimed to develop TiO_2/ZnO coatings with different ZnO contents (wt%). A picoseconds laser ablation technique was used to create dimpled structures on the surfaces of the coatings and the effects of laser surface texturing on the antibacterial properties of the TiO_2/ZnO coatings were investigated. The dimpled patterns were produced to increase the surface area exposed to bacteria and to change the surface topographical properties of the materials. Subsequently, the antibacterial properties of TiO_2/ZnO coatings against *Escherichia coli* were also investigated.

2. Materials and methods

2.1. Preparation of the TiO_2/ZnO coatings

Commercial TiO_2 (Metco 102 Oerlikon Metco, ≥ 99.0 wt%) with a nominal particle size distribution of 11–45 μm and ZnO (Sigma Aldrich, ≥ 99 wt%) with particle size of less than 5 μm were used as raw materials. The TiO_2 and ZnO powders were mixed in the ratios shown in Table 1 and used as feedstock in a plasma spraying process to produce the antibacterial coatings investigated in this study. A polyvinyl alcohol solution (5 wt%) was added into a tank as a binder. The powders were milled for 2 h, dried at 80 °C for 24 h and sieved using an 80-mesh sieve. Then, the coatings were deposited onto grade B API 5L carbon steel with dimensions of 30 cm (length) × 5 cm (width) × 7 mm (thickness) by an atmospheric plasma spray system with a SG-100 torch (Praxair, USA) mounted on an ABB IRB industrial robot. Prior to deposition, the substrate was blasted with aluminium grit (24 mesh) to increase surface roughness and promote mechanical interlocking between the coating and the substrate. Next, the grit-blasted substrates were ultrasonically cleaned in ethanol and deionised water. The dried substrate was

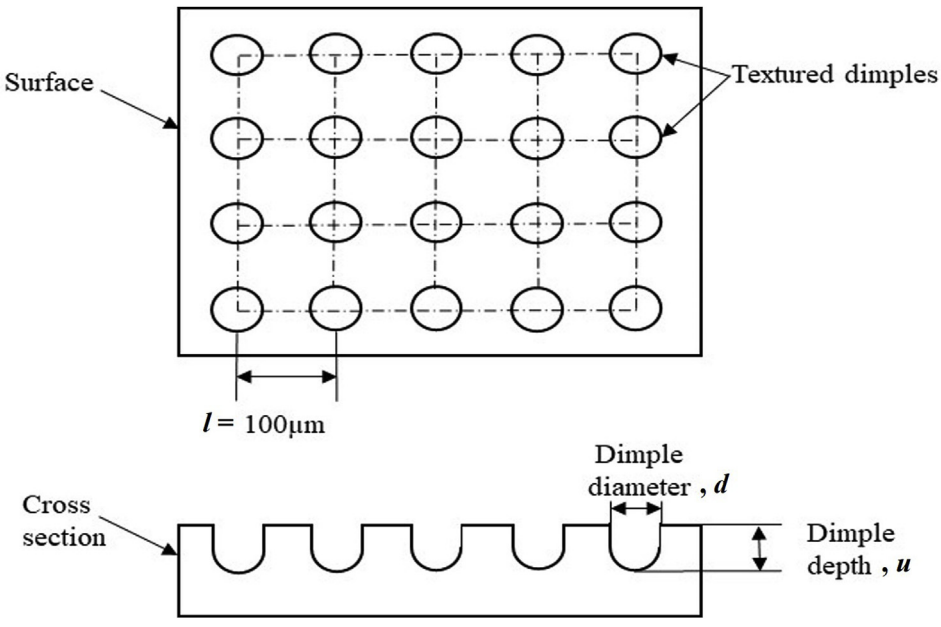

Fig. 1. Schematic of the texturing pattern.

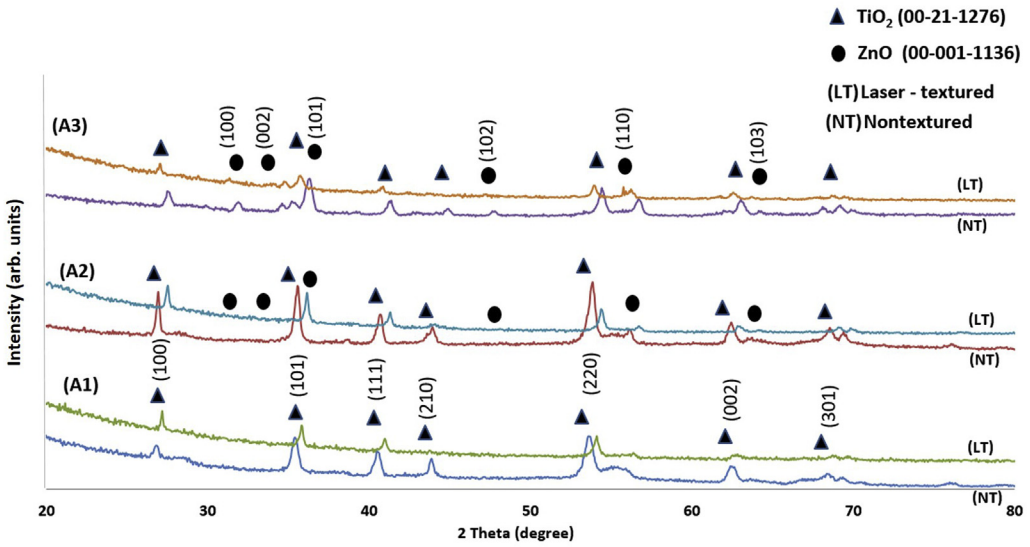

Fig. 2. XRD patterns of the laser surface textured (LT) and non-textured (NT) TiO_2/ZnO coating at different mixing ratio.

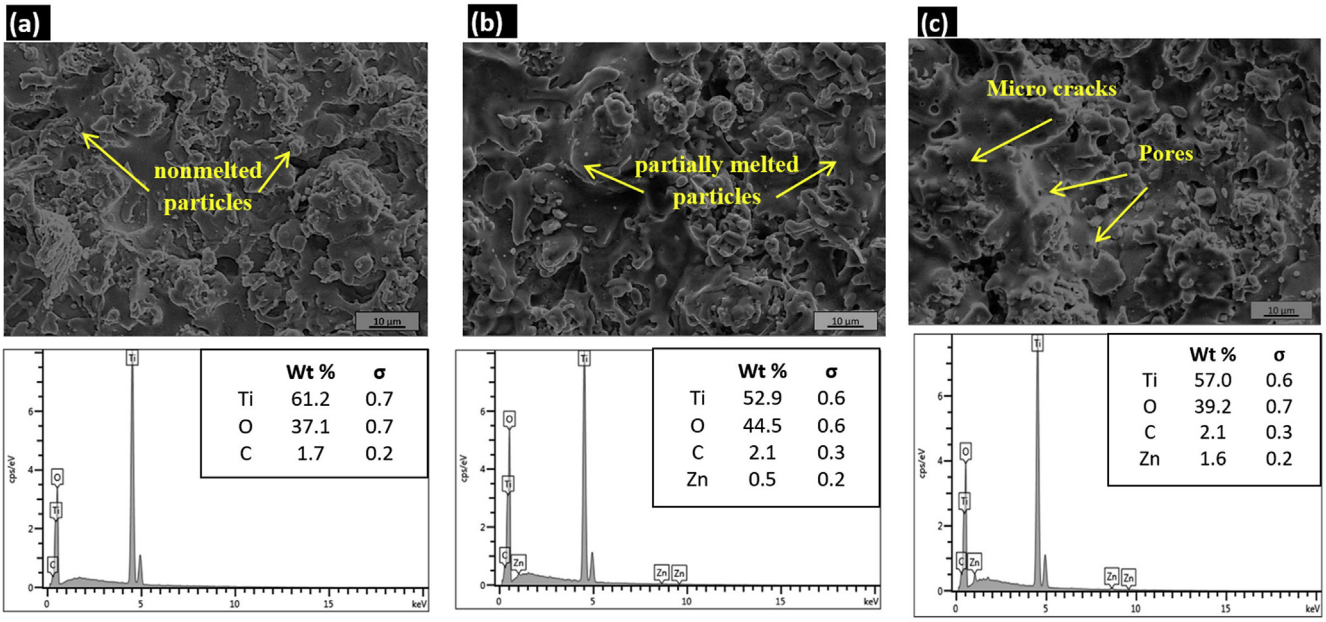

Fig. 3. Surface SEM images and EDX analysis of TiO_2/ZnO coatings with different ZnO contents (a) A1, (b) A2 and(c) A3.

plasma-sprayed under the parameters presented in Table 2. The phases of all the obtained coatings were analysed by X-ray diffraction (XRD, Xpert-Pro system) with CuKα radiation at λ = 1.5406 Å. The XRD patterns were recorded over a 2θ range of 20°–80° at a scan step size of 0.05°. The surface morphologies and elemental compositions of the coatings were observed by scanning electron microscopy (SEM, Zeiss Leo 1450VP) at an accelerating voltage of 15.0 kV and energy dispersive X-ray (EDX, Zeiss Merlin field emission SEM) analysis.

2.2. Laser surface texturing

Plasma-sprayed TiO_2/ZnO ceramic coatings with areas of 8 mm × 8 mm on were subjected to laser surface texturing. A Q-switched Nd:YAG picosecond laser system was used to create micro-dimpled surface textures on the TiO_2/ZnO coatings. As illustrated in Fig. 1, the texturing technique involved covering a series of intermediate lines with dimples by applying a laser with a wavelength of 532 nm and a power of 1 W. Scanning was repeated for 2000 shots per point to produce a dimple. Non-textured samples were used for comparison to measure the effectiveness of the textured samples. XRD, SEM and EDX analyses of the textured samples were performed the same equipment as that described previously. The diameters and depths of the obtained dimples were measured using a Keyence VHX-1000 digital microscope with a 900 × magnification. The increase in the laser-textured surface contact areas and the dimple density were determined using Equations (1) and (2) [30], respectively.

$$\text{Increase in surface contact area} = \frac{\sum(\pi du)i}{\textit{Surface area}} \times 100\% \quad (1)$$

$$\text{Dimple density} = \frac{\pi d^2}{4l^2} \quad (2)$$

where d is dimple diameter, u is the depth, i is the number of dimples and l is the distance between two dimples.

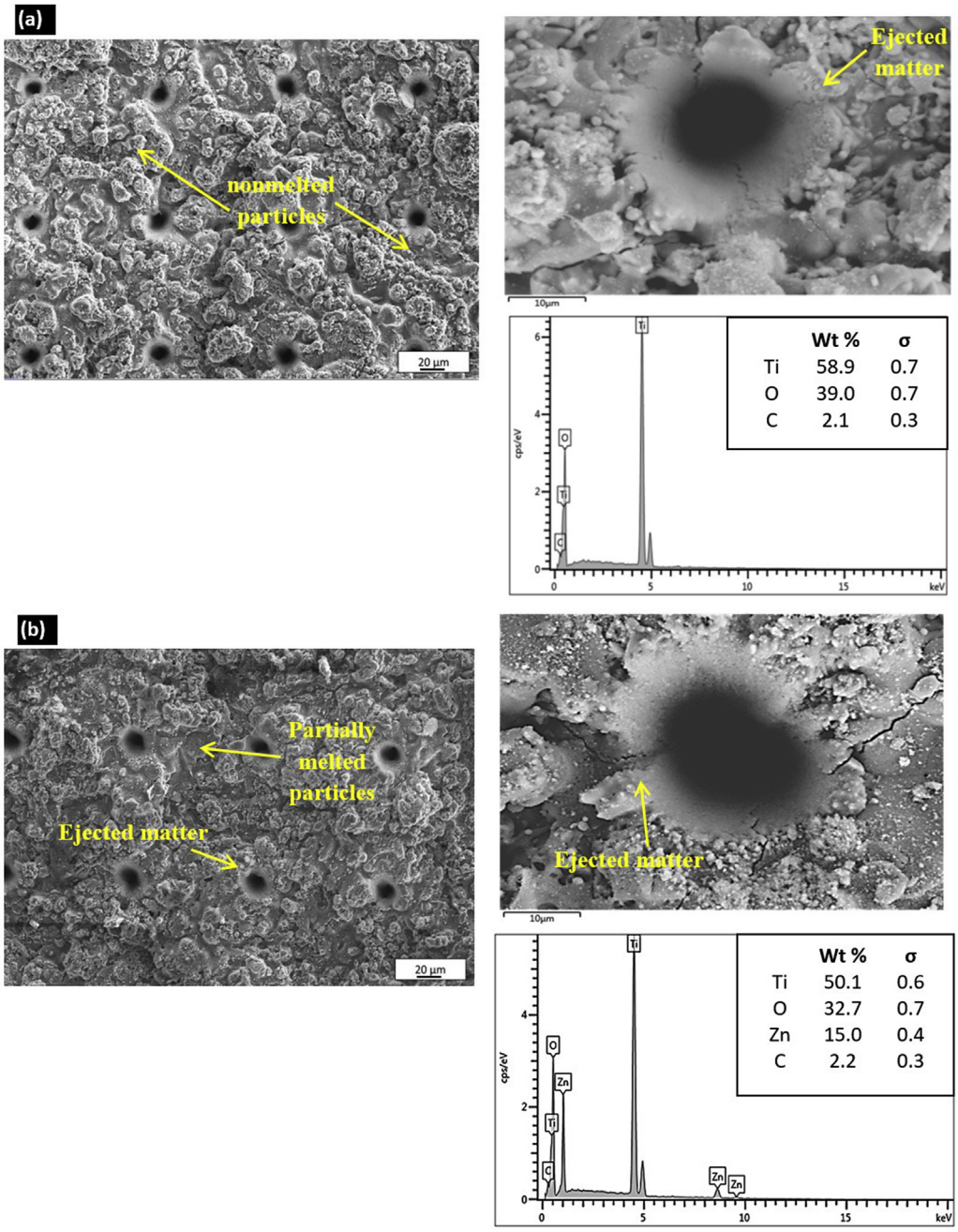

Fig. 4. SEM images and EDX analysis of generated dimple area of laser surface-textured TiO_2/ZnO coatings with different ZnO contents (a) A1, (b) A2 and (c) A3.

2.3. Antibacterial testing

2.3.1. Medium preparation

A bacterial growth medium (nutrient broth/agar) was prepared by dissolving bactoyeast (0.5 wt %), tryptone (10 wt %) and NaCl (10 wt %) in ion-free water in accordance with the Luria–Bertani (LB), Miller broth medium preparation protocol. Then, the medium was sterilised in an autoclaved at 120 °C at 15 psi for 20 min. Bacterial suspensions were prepared by diluting high concentrations of bacterial cultures in the prepared medium.

2.3.2. Bacterial cultures

The bacterial cultures of the *Escherichia coli* (*E. coli*) K12 strain used in this study were supplied by Nihon Freezer Co. Ltd. (Japan). The initial concentration of the *E. coli* suspension was 10^6 colony-forming units (CFU)/ml in accordance with the JIS Z 28015.2 standard.

2.3.3. Bacterial growth evaluation

Bacterial growth on the substrates was determined by measuring the turbidity of the *E.coli* suspension or also known as the optical density (OD). Square pieces of the textured and non-textured coatings with dimensions of 8 mm × 8 mm were used in this test. Prior to the test, all samples were cleaned and sterilised in an ultrasonic 99.9% ethanol bath for 20 min and then rinsed three times with ethanol to remove dirt and dissolve nonreacted ligands on the surfaces of the samples. The immersed samples were placed in 5 ml of *E. coli* suspension. The *E. coli* suspension was incubated at 37 °C at a vibration frequency of 170/min for 1 h. The OD values of the *E. coli* suspension were determined every 1 h for 3 h after the initiation of the experiment using a spectrophotometer (Hitachi Technologies U-1100, Japan). OD values were determined on the basis of the ratio of the intensity of light transmitted through a culture medium (I_o) to the intensity of light transmitted through a culture medium containing *E. coli* (I_{CM}) as shown in Equation

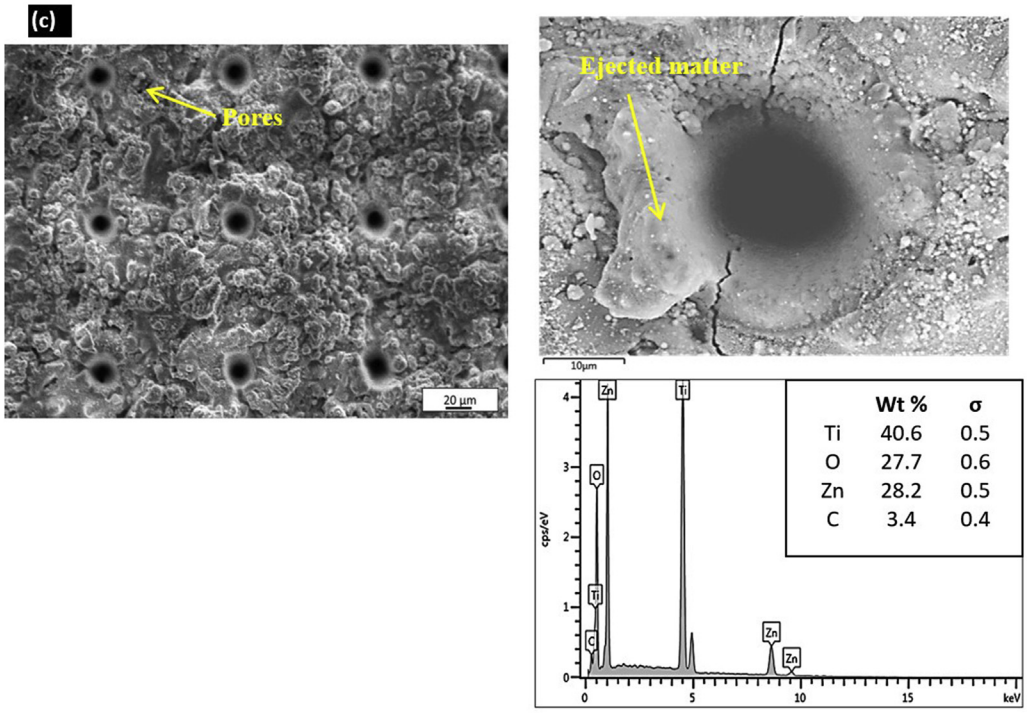

Fig. 4. (*continued*)

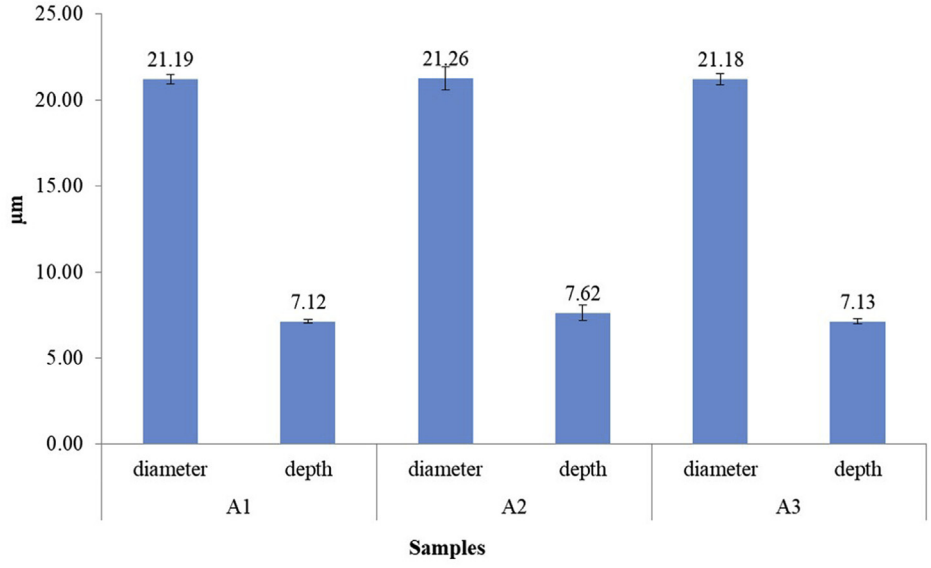

Fig. 5. Average diameter and depth of dimples produced by laser surface texturing the coatings.

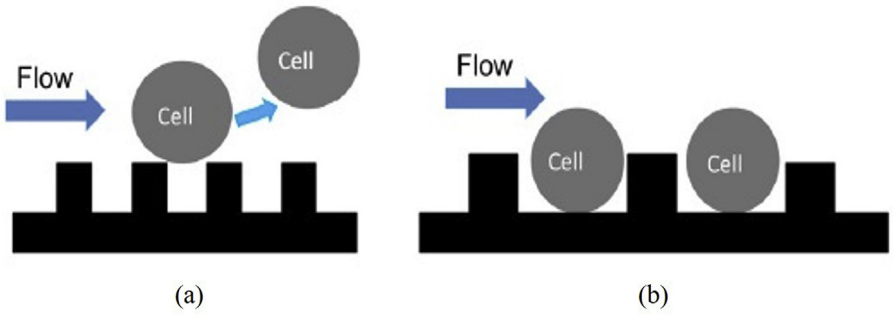

Fig. 6. Schematic diagram of bacterial adhesion on (a) submicron-textured and (b) microtextured surfaces [38].

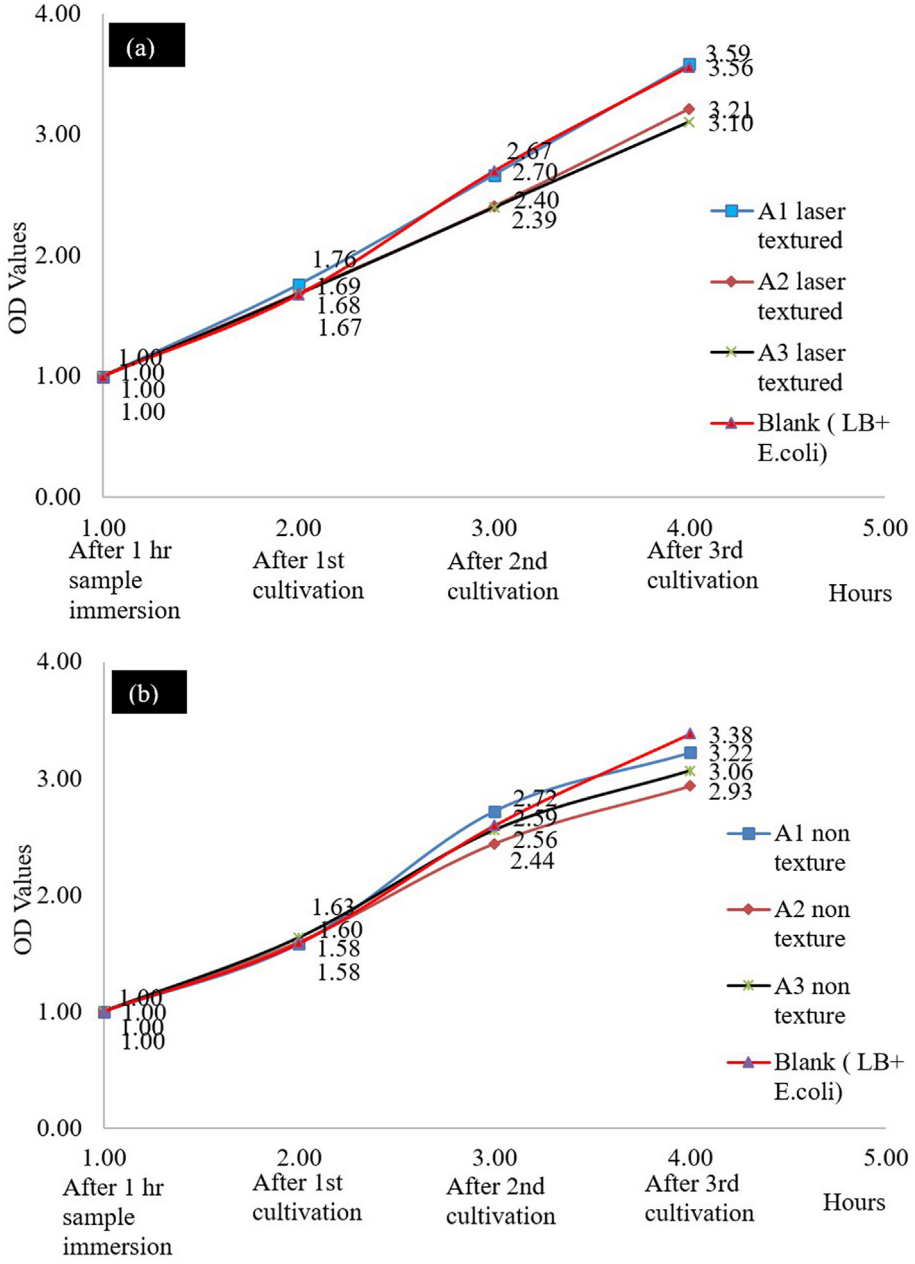

Fig. 7. Changes in the normalised OD of (a) laser surface-textured and (b) non-textured A1–A3 samples.

(3). The OD values were normalised with respect to the value obtained at the initial time point for each sample. E.coli in the LB culture medium without sample immersion was used as the blank sample for comparison purposes.

$$OD = \frac{\log(I_{CM,t=i}/Io)}{\log(I_{CM,t=o}/Io)}, \quad \text{where} \quad i = 1,2,3\ldots \text{ (hours)} \tag{3}$$

2.3.4. Bacterial plate count

The CFUs was used to estimate the number of viable bacteria in a sample. In this study, a 10^{-4} dilution of *E. coli* suspension was prepared by using the culture medium after sample immersion and incubation at 37 °C for 1 h. Then, 0.1 ml of the diluted suspension was grown on agar at 37 °C for 18 h. The colonies on the nutrient agar culture medium were counted from photographs in accordance with the USDA standard (BBSOP0019.04).

2.3.5. Bacterial viability test

Bacterial viability assays are widely used to evaluate antibacterial properties and assess the susceptibility of bacteria to biocides. In this study, the adhesion and viability of *E. coli* on the surfaces of the textured and non-textured coatings were observed using a fluorescence microscope (BZ-8100, Keyence Co., Ltd). The *E. coli* nuclei were stained using the SYTO 9 stain from Thermo Fisher Scientific Inc. followed the instructions provided with the stain for quantitative analyses prior to microscopy.

3. Results and discussion

3.1. XRD patterns and microstructures of non-textured TiO_2/ZnO ceramic coatings

Fig. 2 shows the XRD patterns of the coatings containing only TiO_2 (A1), 90 wt% TiO_2 with 10 wt% ZnO (A2) and 70 wt% TiO_2 with 30% ZnO (A3). The A1 XRD pattern showed peaks associated with the (110),

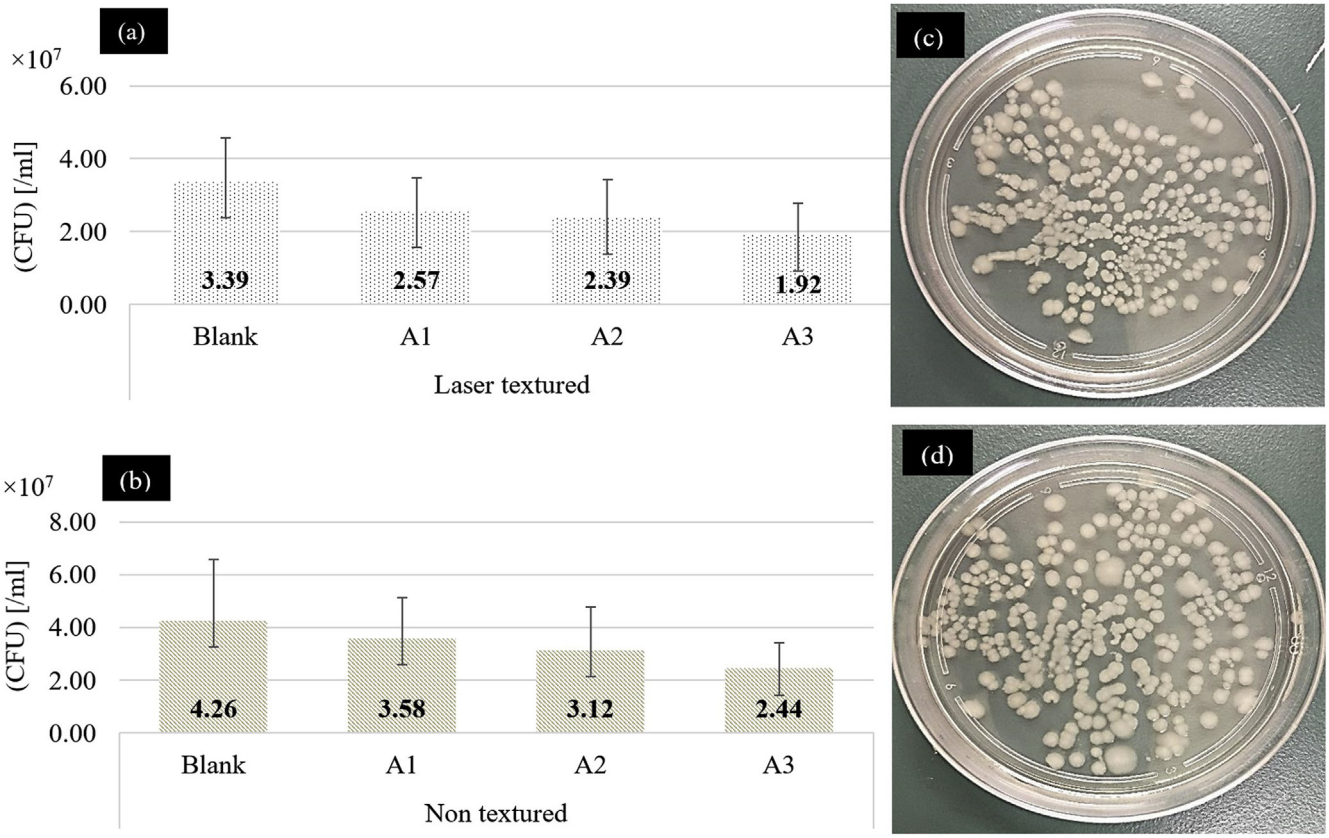

Fig. 8. The number of CFUs on (a) laser surface -textured and (b) non-textured TiO_2/ZnO coatings. Representative images are also shown of *E. coli* recultivated on agar from suspensions of (c) laser-textured and (d) non-textured TiO_2/ZnO coatings.

(101), (111) and (210) planes, which are consistent with rutile titania (JCPDS 00-21-1276). The XRD peaks for A2 and A3 shifted to a low angle because of the introduction of ZnO into the TiO_2 lattice without rutile phase alteration (Fig. 2). The sharp diffraction peaks in the spectra are indicative of high TiO_2 crystallinity, which can be attributed to high purity. The reduction in the intensity of the major TiO_2 diffraction peak in the XRD spectra of A3 when the ZnO content was increased to 30 wt% suggests that ZnO phases were present without rutile phase alteration [31]. The low-intensity ZnO peaks in the XRD spectra of A2 were mainly attributed to the low ZnO content of the sample.

Fig. 3 displays the SEM images of the TiO_2/ZnO ceramic coatings prepared with different ZnO contents. The coatings present the typical microroughened surfaces that are characteristic of plasma spraying products. The as-sprayed coating (Fig. 3a–c) contained partially melted and nonmelted particles that had adhered to fully melted splats. Semi-spherical and spherical particles corresponded to partially melted and nonmelted particles, respectively (Fig. 3b). Several surface microcracks formed as the ZnO content of the coatings increased. For example, there were more microcracks and pores in the surface of A3 (Fig. 3c) compared to in the surface of A1 or A2 that contained less ZnO. Microcrack formation could be attributed to the combination of the reinforcement of the TiO_2/ZnO and nonmelted particles. Similarly, Zhao et al. [31] observed that TiO_2 coatings with the highest ZnO content showed irregular and disordered morphologies due to the high-temperature characteristic of plasma spraying and rapid cooling rates.

3.2. XRD analysis, morphology and structural characterisation of laser surface-textured TiO_2/ZnO ceramic coatings

Picosecond laser ablation was used to create dimples on the surfaces of the TiO_2/ZnO ceramic coatings. The XRD patterns of the laser surface-textured A1, A2 and A3 coatings are shown in Fig. 2. The XRD peaks of the laser surface-textured coatings shifted to a slight higher angle of 2θ compared to non-textured samples. Usually, peak shifts to higher angles is attributed to stress and defect relaxation that occur in coatings after the coatings are annealed at a temperature that is higher than the deposition temperature [32]. In this case, the increased temperature during the laser ablation process is believed to be the main reason for the peak shift. The sharp diffraction peaks observed in the patterns of the laser surface-textured samples had reduced intensities compared to the non-textured samples. The decrease in the intensity of the major TiO_2 and ZnO diffraction peaks in the XRD spectra of the laser surface-textured A2 and A3 samples suggest that no phase alteration occurred. However, the different peak shapes correspond to the preferential growth of different crystal planes, which resulted in XRD peaks with different intensities [32].

SEM was used to observe the overall surface features of the laser surface-textured samples, and the results shown in Fig. 4 indicate that macroporous structures remained after laser texturing. The SEM images (Fig. 4a–c) revealed that samples showed melted and nonmelted particles combined with pores and cracks observed on the surface. The areas surrounding the dimples were covered with matter ejected during the dimple formation (Fig. 4a–c). The temperature of the material increases during the laser–material interaction and the material begins to melt; ejection occurs on the surface as a result of the ensuing pressure drop [33]. The EDX analyses (Fig. 4a–c) of the generated dimples area show that distinct oxygen peaks were detected beside titanium and zinc. This is because the surface layers of the samples oxidized when exposed to air and high temperature during laser surface texturing process. We also analysed the surface chemistry of the samples after texturing. For example, the Ti and O content of A1 was determined to contain 61.2 ± 0.7 wt % Ti and 37.1 ± 0.7 wt % O before surface texturing and 58.9 ± 0.7 wt % Ti and 39.0 ± 0.7 wt % O after texturing, which means the picosecond laser process did not affect the

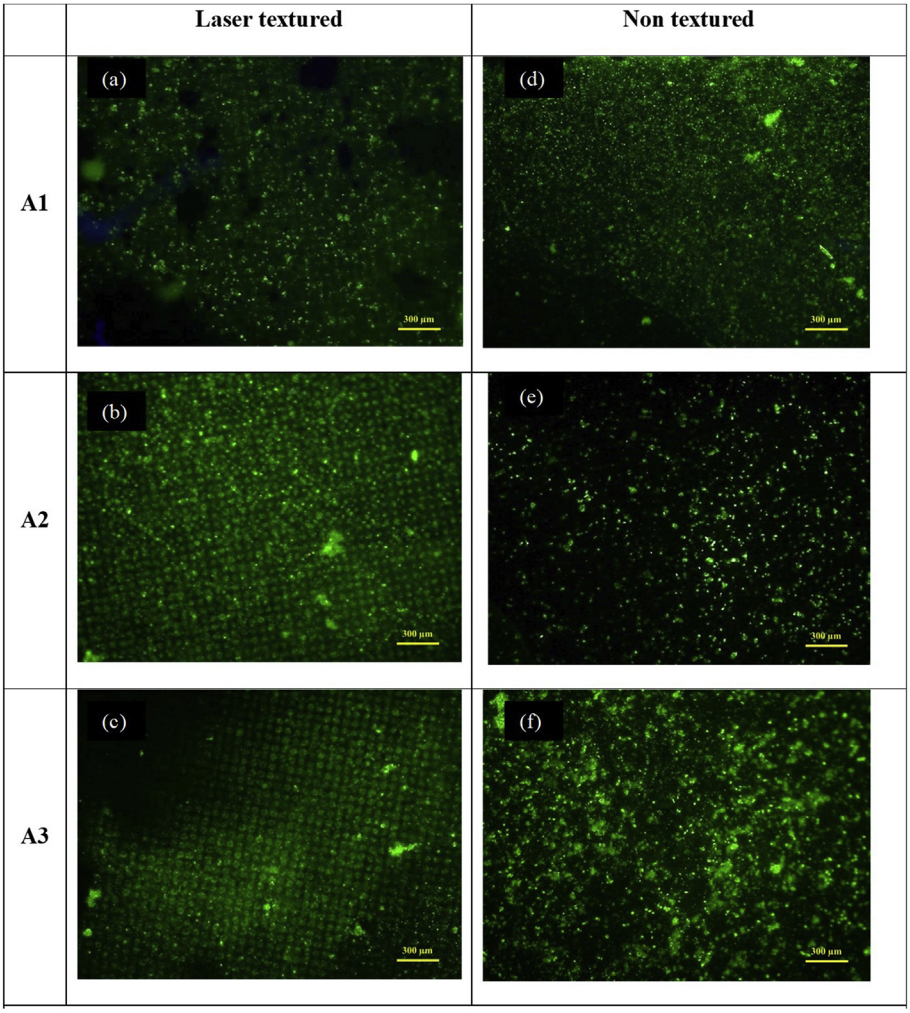

Fig. 9. SYTO 9-stained live cell bacteria on laser-textured (a) A1, (b) A2 and (c) A3 coatings and non-textured(d) A1, (e) A2 and (f) A3 coatings.

surface chemistry of A1 significantly.

A digital microscope was used to measure the diameters and depths of the dimples generated by laser texturing. The average diameters and depths of the dimples in all samples were on average 21.21 ± 0.33 and 7.29 ± 0.21 µm, respectively, as shown in Fig. 5. These values showed that laser texturing increased the total initial surface contact area of the coating by more than approximately 5 % with a dimple density of 3.5 %. Increasing the contact area of a solid surface exposes more of its material to potential chemical and/or physical interactions, which increases the chance of collisions between the surface and other particles and can increase reaction rates. The availability of surface contact area is also one of the main factors that influence bacterial adhesion [34,35]. Shaikh *et. al* [5] reported that laser surface modification enhances bacterial rejection without affecting the biocompatibility of surfaces. Surface textural features that are smaller than bacterial cells inhibit bacterial adhesion by reducing the available surface contact area between bacteria and the surface (Fig. 6a) [23,36]. Meanwhile, surfaces with textural features that are comparable in size with the size of a bacterial cell, i.e., micron-sized features, facilitate bacterial access into spaces between textural features (Fig. 6b) as bacteria tend to align and maximise their contact area with the surface. This tendency results in different adhesion behaviours that are dependent on the shape, size, chemical composition and wettability of the surface [6,37,38].

3.3. Antibacterial activity of TiO_2/ZnO coatings

The bacterial growth on the laser textured and non-textured samples is shown in Fig. 7. The degree of culture medium turbidity is directly related to the number of microorganisms present. Thus, the culture medium turbidity increases as the microbial cell mass increases. Fig. 7 shows that the addition of ZnO strongly affected the OD slopes, particularly those of the laser textured surfaces (Fig. 7a). The OD value of the laser surface-textured samples differed significantly with increasing ZnO content at each cultivation time point. For example, as illustrated in Fig. 7a, the laser surface-textured A3 coating consistently yielded the lowest OD value at each cultivation time point. The antibacterial properties of the laser surface-textured TiO_2/ZnO coatings were therefore associated with the ZnO content. The laser surface-textured A2 and A3 coatings were associated with a significant reduction in the bacterial growth at each cultivation time point. Meanwhile, no significant trend was observed in the bacterial growth of the non-textured coatings (Fig. 7b). The non-textured coatings lacked significant antibacterial properties regardless of ZnO contents and provided inconsistent OD values at different cultivation time points. For example, the highest OD value for the non-texturedA3 coating was obtained after the first cultivation time point. Nevertheless, the OD values of the same coating at the second and third cultivation time points decreaed. These results indicate that texturing enhanced the antibacterial properties of the TiO_2/ZnO coatings and that texturing enhanced the antibacterial properties of ZnO and TiO_2.

Furthermore, the numbers of CFUs on the laser surface-textured TiO_2/ZnO coatings were lower than those on the non-textured coatings (Fig. 8a–b). For example, the number of CFUs on the laser surface-textured A1 sample was approximately 24.2 % lower than that on the

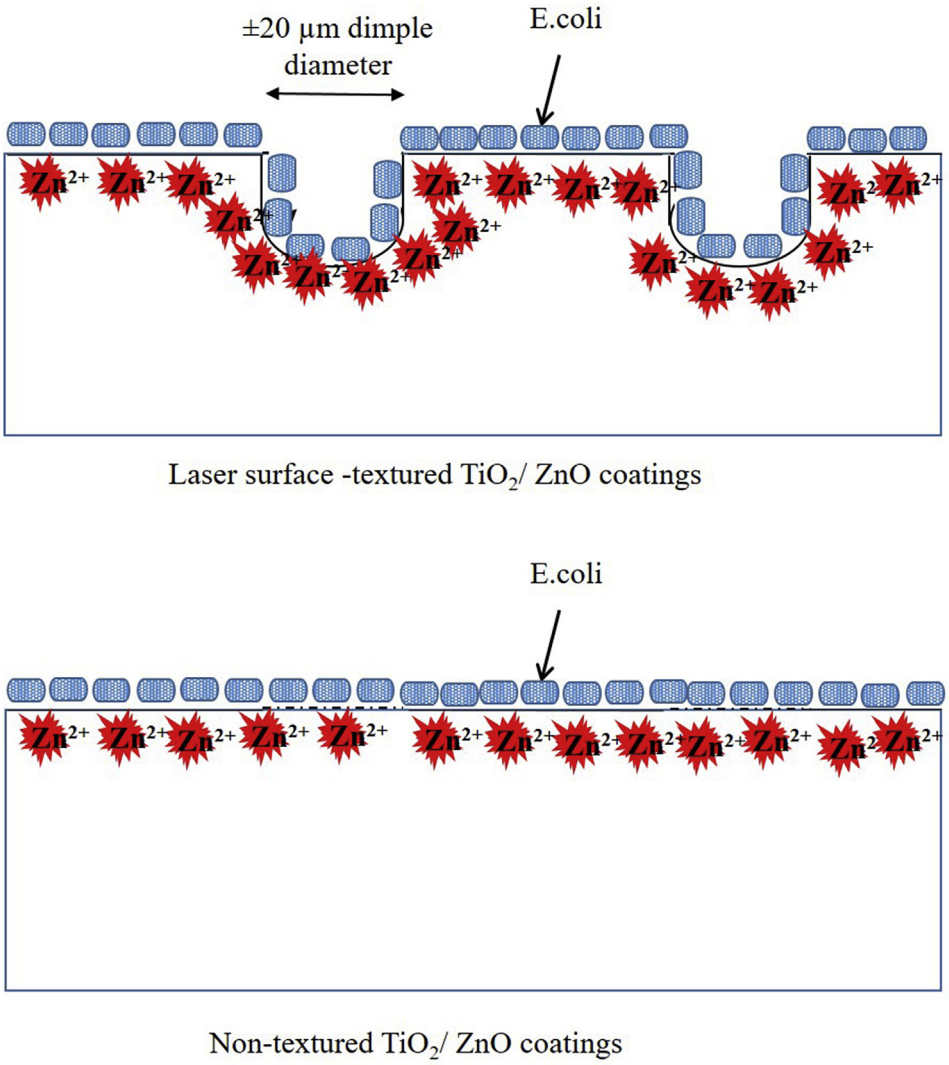

Fig. 10. Schematic diagram showing the enhancement of bacterial attachment on surface-textured TiO_2/ZnO coatings; Zn^{2+} from ZnO inhibits the bacterial growth resulting in bacterial death.

blank sample, whereas that on the non-texturedA1 sample was only approximately 15.9 % lower than that on the blank sample. These results show that laser texturing the surfaces improved the antibacterial properties of the TiO_2/ZnO coatings. Furthermore, the number of CFUs decreased significantly when the ZnO content increased. This reduction in CFUs showed that ZnO in the coatings influenced the antibacterial properties of the laser surface-textured and non-textured surfaces.

The amount of viable *E. coli* grown on the laser surface-textured and non-texturedTiO$_2$/ZnO coatings are shown in Fig. 9. Notably, laser texturing improved the antibacterial properties of the TiO_2/ZnO coatings, which indicates that the laser surface-textured coatings had a higher antibacterial activity than the non-textured coatings. Bacterial growth was uninhibited in samples with non-textured surfaces (Fig. 9d–f) but was inhibited on the laser surface textured coatings (Fig. 9a–c). The fluorescence images indicate that few *E. coli* bacteria were present on the laser surface-textured coatings. Furthermore, fewer bacteria were observed on the laser surface-textured A3 sample than on the laser surface-textured A2 and A1 samples. However, the number of bacteria detected on non-texturedTiO$_2$/ZnO coatings (Fig. 9d–f) was not significantly correlated to the ZnO content of the coating. This result is consistent with the OD value measurements and the number of CFUs, and demonstrates that the laser surface-textured TiO_2/ZnO coatings have antibacterial properties. These results can be attributed to two reasons.

(i) Zn exhibits inhibitory and antimicrobial effects on various types of bacteria [15,39]. Zn also has bacteriostatic properties, for example Zn^{+2} ions can influence the growth of various bacteria when released [12]. Furthermore, the incorporation of Zn can enhance the antibacterial activity and biocompatibility of TiO_2 coatings. ZnO acts as an efficient antibacterial agent by destabilising bacterial membranes upon coming into direct contact with bacteria [12,39,40].

(ii) The dimples formed in the TiO_2/ZnO ceramic coatings increased the surface area of the coating by more than 5 %, which also increased the amount of TiO_2 and ZnO exposed as antibacterial agents. *E. coli* bacterial cells are typically approximately 2.0 µm long rod-shapes with a diameter of 0.25–1.0 µm [23]. The fact that the *E.coli* bacteria were smaller than the dimples increased the bacterial adhesion on the textured surfaces. Bacterial adhesion on regularly patterned microscale features, such as grooves and pits (dimples), are able to trap and localize the *E.coli* cells and thereby direct the bacterial attachment to surfaces [41]. The attachment of *E. coli* bacteria on laser -textured surfaces leads to cell cycle arrest and death. Zn^{2+} from ZnO can inhibit bacterial growth by penetrating the cell wall, which results in bacterial death [42]. Zn^{2+} can also act as a catalytically active centre producing hydroxyl radicals that damage the reproductive capacity of the bacteria, which leads to bacterial death [42]. This finding is consistent with that of this

study, in which bacterial attachment on TiO_2/ZnO coatings with non-textured surfaces was high regardless of ZnO content as evinced by the strong green fluorescence signal in Fig. 9d–f. On the other hand, the green fluorescence signal Fig. 9a–c was relatively weak, which indicates that the most of the bacteria lost their viability on the laser-textured surfaces.

In this work, the introduction of ZnO into TiO_2 ceramic coatings by plasma spraying resulted in coatings with high antibacterial activity. The effectiveness of ZnO as an antibacterial agent can be observed in the samples with laser-textured surfaces. As illustrated in Fig. 10, increasing the surface area of the TiO_2/ZnO coatings by laser surface texturing promoted bacterial attachment to the surface coating; the dimples, which were larger than bacterial cells, provided additional spaces for bacterial attachment. The increase in bacterial attachment on the surface coating helped facilitate the action of ZnO and TiO_2 as antibacterial agents as evinced by the OD measurements, the numbers of CFUs on each sample and the fluorescence imaging results. All the results indicate that laser surface texturing increased the antibacterial properties of the TiO_2/ZnO coatings.

4. Conclusions

We used a picosecond laser to texture the surfaces of TiO_2/ZnO ceramic coatings with different ZnO contents and investigated their antibacterial properties. The results showed that the presence of dimples on the surface drastically affected the antibacterial properties of the TiO_2/ZnO coatings. The laser surface-textured coatings had lower ODs, fewer CFUs and less live cell bacteria as observed by fluorescence microscopy than the non-textured samples. Increasing the surface area of the TiO_2/ZnO coating by laser surface texturing promoted bacterial attachment to the surface coating. The increase in bacterial attachment on the surface coating helped facilitate the action of ZnO and TiO_2 as antibacterial agents.

Declaration of competing interest

The authors declare that they have no known competing financial interests or personal relationships that could have appeared to influence the work reported in this paper.

Acknowledgements

This work was supported by the Ministry of Higher Education Malaysia and Universiti Kebangsaan Malaysia (grant number FRGS/1/2018/TK03/UKM/02/8). The authors also thank Nagaoka University of Technology, Japan and JASSO Scholarship for their support and cooperation during the experiments. The first author also acknowledges Universiti Teknikal Malaysia Melaka for financially supporting her Ph.D. study.

Appendix A. Supplementary data

Supplementary data to this article can be found online at https://doi.org/10.1016/j.ceramint.2019.10.124.

References

[1] L.D. Chambers, K.R. Stokes, F.C. Walsh, R.J.K. Wood, Modern approaches to marine antifouling coatings, Surf. Coat. Technol. 201 (2006) 3642–3652, https://doi.org/10.1016/j.surfcoat.2006.08.129.
[2] H.M. Page, J.E. Dugan, F. Piltz, Fouling and antifouling in oil and other offshore industries, Biofouling (2010) 252–266.
[3] I. Banerjee, R.C. Pangule, R.S. Kane, Antifouling coatings: recent developments in the design of surfaces that prevent fouling by proteins, bacteria, and marine organisms, Adv. Mater. 23 (2011) 690–718, https://doi.org/10.1002/adma.201001215.
[4] F.H. Rajab, C.M. Liauw, P.S. Benson, L. Li, K.A. Whitehead, Production of hybrid macro/micro/nano surface structures on Ti6Al4V surfaces by picosecond laser surface texturing and their antifouling characteristics, Colloids Surf., B 160 (2017) 688–696, https://doi.org/10.1016/j.colsurfb.2017.10.008.
[5] S. Shaikh, D. Singh, M. Subramanian, S. Kedia, A.K. Singh, K. Singh, N. Gupta, S. Sinha, Femtosecond laser induced surface modification for prevention of bacterial adhesion on 45S5 bioactive glass, J. Non-Cryst. Solids 482 (2018) 63–72, https://doi.org/10.1016/j.jnoncrysol.2017.12.019.
[6] K.A. Whitehead, J. Colligon, J. Verran, Retention of microbial cells in substratum surface features of micrometer and sub-micrometer dimensions, Colloids Surf., B 41 (2005) 129–138, https://doi.org/10.1016/j.colsurfb.2004.11.010.
[7] L. Costa, D.M. Dantas, J.P. Silva-neto, T.S. Dantas, L.Z. Naves, F. Domingues, A. Soares, Bacterial adhesion and surface roughness for different clinical techniques for acrylic polymethyl methacrylate, Int. J. Dentistry 2016 (2016) 8685796, https://doi.org/10.1155/2016/8685796.
[8] G. Zhao, W.N. Chen, Biofouling formation and structure on original and modified PVDF membranes: role of microbial species and membrane properties, RSC Adv. 7 (2017) 37990–38000, https://doi.org/10.1039/C7RA04459C.
[9] H. Wang, H. Feng, W. Liang, Y. Luo, V. Malyarchuk, Effect of surface roughness on retention and removal of Escherichia coli O157:H7 on surfaces of selected fruits, J. Food Sci. 74 (2009) 1–8, https://doi.org/10.1111/j.1750-3841.2008.00998.x.
[10] F. Robotti, S. Bottan, F. Fraschetti, A. Mallone, G. Pellegrini, N. Lindenblatt, C. Starck, V. Falk, D. Poulikakos, A. Ferrari, A micron-scale surface topography design reducing cell adhesion to implanted materials, Sci. Rep. 8 (2018) 10887, https://doi.org/10.1038/s41598-018-29167-2.
[11] E. Fadeeva, V.K. Truong, M. Stiesch, B.N. Chichkov, R.J. Crawford, J. Wang, E.P. Ivanova, Bacterial retention on superhydrophobic titanium surfaces fabricated by femtosecond laser ablation, Langmuir 27 (2011) 3012–3019, https://doi.org/10.1021/la104607g.
[12] R. Zhang, X. Liu, Z. Xiong, Q. Huang, X. Yang, H. Yan, J. Ma, Q. Feng, Z. Shen, Novel micro/nanostructured TiO2/ZnO coating with antibacterial capacity and cytocompatibility, Ceram. Int. 44 (2018) 9711–9719, https://doi.org/10.1016/j.ceramint.2018.02.202.
[13] D. Campoccia, L. Montanaro, C.R. Arciola, A review of the biomaterials technologies for infection-resistant surfaces, Biomaterials 34 (2013) 8533–8554, https://doi.org/10.1016/j.biomaterials.2013.07.089.
[14] K. Siwińska-Stefańska, A. Kubiak, A. Piasecki, J. Goscianska, G. Nowaczyk, S. Jurga, T. Jesionowski, TiO2-ZnO binary oxide systems: comprehensive characterization and tests of photocatalytic activity, Materials 11 (2018) 841, https://doi.org/10.3390/ma11050841.
[15] X. Zhao, J. Yang, J. You, Surface modification of TiO2coatings by Zn ion implantation for improving antibacterial activities, Bull. Mater. Sci. 39 (2016) 285–291, https://doi.org/10.1007/s12034-015-1127-1.
[16] B.S. Yilbas, M. Khaled, N. Abu-Dheir, N. Aqeeli, S.Z. Furquan, Laser texturing of alumina surface for improved hydrophobicity, Appl. Surf. Sci. 286 (2013) 161–170, https://doi.org/10.1016/j.apsusc.2013.09.040.
[17] H. Yan, M.R.B. Abdul Rashid, S.Y. Khew, F. Li, M. Hong, Wettability transition of laser textured brass surfaces inside different mediums, Appl. Surf. Sci. 427 (2018) 369–375, https://doi.org/10.1016/j.apsusc.2017.08.218.
[18] V.D. Ta, A. Dunn, T.J. Wasley, J. Li, R.W. Kay, J. Stringer, P.J. Smith, E. Esenturk, C. Connaughton, J.D. Shephard, Laser textured superhydrophobic surfaces and their applications for homogeneous spot deposition, Appl. Surf. Sci. 365 (2016) 153–159, https://doi.org/10.1016/j.apsusc.2016.01.019.
[19] J.I. Ahuir-Torres, M.A. Arenas, W. Perrie, G. Dearden, J. de Damborenea, Surface texturing of aluminium alloy AA2024-T3 by picosecond laser: effect on wettability and corrosion properties, Surf. Coat. Technol. 321 (2017) 279–291, https://doi.org/10.1016/j.surfcoat.2017.04.056.
[20] A.Y. Vorobyev, C. Guo, Multifunctional surfaces produced by femtosecond laser pulses, J. Appl. Phys. 117 (2015) 033103, , https://doi.org/10.1063/1.4905616.
[21] A.G. Demir, P. Maressa, B. Previtali, Fibre laser texturing for surface functionalization, Physics Procedia 41 (2013) 759–768, https://doi.org/10.1016/j.phpro.2013.03.145.
[22] V.D. Ta, A. Dunn, T.J. Wasley, J. Li, R.W. Kay, J. Stringer, P.J. Smith, E. Esenturk, C. Connaughton, J.D. Shephard, Laser textured surface gradients, Appl. Surf. Sci. 371 (2016) 583–589, https://doi.org/10.1016/j.apsusc.2016.03.054.
[23] M. Lorenzetti, I. Dogša, T. Stošicki, D. Stopar, M. Kalin, S. Kobe, S. Novak, The influence of surface modification on bacterial adhesion to titanium-based substrates, ACS Appl. Mater. Interfaces 7 (2015) 1644–1651, https://doi.org/10.1021/am507148n.
[24] M.V. Graham, A.P. Mosier, T.R. Kiehl, A.E. Kaloyeros, N.C. Cady, Development of antifouling surfaces to reduce bacterial attachment, Soft Matter 9 (2013) 6235–6244, https://doi.org/10.1039/C3SM50584G.
[25] F.H. Rajab, Z. Liu, T. Wang, L. Li, Controlling bacteria retention on polymer via replication of laser micro/nano textured metal mould, Opt. Laser. Technol. 111 (2019) 530–536, https://doi.org/10.1016/j.optlastec.2018.10.031.
[26] C.W. Chan, L. Carson, G.C. Smith, A. Morelli, S. Lee, Enhancing the antibacterial performance of orthopaedic implant materials by fibre laser surface engineering, Appl. Surf. Sci. 404 (2017) 67–81, https://doi.org/10.1016/j.apsusc.2017.01.233.
[27] F.H. Rajab, C.M. Liauw, P.S. Benson, L. Li, K.A. Whitehead, Picosecond laser treatment production of hierarchical structured stainless steel to reduce bacterial fouling, Food Bioprod. Process. 109 (2018) 29–40, https://doi.org/10.1016/j.fbp.2018.02.009.
[28] X. Ge, Y. Leng, X. Lu, F. Ren, K. Wang, Y. Ding, M. Yang, Bacterial responses to periodic micropillar array, J. Biomed. Mater. Res. A 103 (2015) 384–396, https://doi.org/10.1002/jbm.a.35182.
[29] J. Valle, S. Burgui, D. Langheinrich, C. Gil, C. Solano, A. Toledo-Arana, R. Helbig, A. Lasagni, I. Lasa, Evaluation of surface microtopography engineered by direct

laser interference for bacterial anti-biofouling, Macromol. Biosci. 15 (2015) 1060–1069, https://doi.org/10.1002/mabi.201500107.
[30] Y.L. Zhang, X.G. Zhang, G. Matsoukas, Numerical study of surface texturing for improving tribological properties of ultra-high molecular weight polyethylene, Biosurf. Biotribol. 1 (2015) 270–277, https://doi.org/10.1016/j.bsbt.2015.11.003.
[31] X. Zhao, C. Peng, J. You, Plasma-sprayed ZnO/TiO_2 coatings with enhanced biological performance, J. Therm. Spray Technol. 26 (2017) 1301–1307, https://doi.org/10.1007/s11666-017-0573-2.
[32] N. Iwashita, X-ray Powder Diffraction, Material Science and Engineering of Carbon, Tsinghua University Press Limited., 2016, pp. 7–25.
[33] S. Costil, A. Lamraoui, C. Langlade, O. Heintz, R. Oltra, Surface modifications induced by pulsed-laser texturing - influence of laser impact on the surface properties, Appl. Surf. Sci. 288 (2014) 542–549, https://doi.org/10.1016/j.apsusc.2013.10.069.
[34] L.C. Xu, C.A. Siedlecki, Staphylococcus epidermidis adhesion on hydrophobic and hydrophilic textured biomaterial surfaces, Biomed. Mater. 9 (2014) 035003, https://doi.org/10.1088/1748-6041/9/3/035003.
[35] V. Vadillo-Rodríguez, B.E. Logan, Localized attraction correlates with bacterial adhesion to glass and metal oxide substrata, Environ. Sci. Technol. 40 (2006) 2983–2988, https://doi.org/10.1021/es052365v.
[36] G. Feng, Y. Cheng, S.Y. Wang, D.A. Borca-Tasciuc, R.W. Worobo, C.I. Moraru, Bacterial attachment and biofilm formation on surfaces are reduced by small-diameter nanoscale pores: how small is small enough? npj Biofilms Microbiomes 1 (2015) 15022, https://doi.org/10.1038/npjbiofilms.2015.22.
[37] L.C. Hsu, J. Fang, D.A. Borca-Tasciuc, R.W. Worobo, C.I. Moraru, Effect of micro- and nanoscale topography on the adhesion of bacterial cells to solid surfaces, Appl. Environ. Microbiol. 79 (2013) 2703–2712, https://doi.org/10.1128/AEM.03436-12.
[38] L.-C. Xu, C.A. Siedlecki, Surface texturing and control of bacterial adhesion, Compr. Biomater. II. 4 (2017) 303–320, https://doi.org/10.1016/B978-0-12-803581-8.09295-X.
[39] R. Kumar, A. Umar, G. Kumar, H.S. Nalwa, Antimicrobial properties of ZnO nanomaterials: a review, Ceram. Int. 43 (2017) 3940–3961, https://doi.org/10.1016/j.ceramint.2016.12.062.
[40] N. Geetha, S. Sivaranjani, A. Ayeshamariam, J.S. Kissinger, M. Valan Arasu, M. Jayachandran, ZnO doped oxide materials: mini review, Fluid Mech. Open Acc. 03 (2016), https://doi.org/10.4172/2476-2296.1000141.
[41] R.J. Crawford, H.K. Webb, V.K. Truong, J. Hasan, E.P. Ivanova, Surface topographical factors influencing bacterial attachment, Adv. Colloid Interface Sci. 179–182 (2012) 142–149, https://doi.org/10.1016/j.cis.2012.06.015.
[42] S. Pang, Y. He, R. Zhong, Z. Guo, P. He, C. Zhou, B. Xue, X. Wen, H. Li, Multifunctional ZnO/TiO 2 nanoarray composite coating with antibacterial activity, cytocompatibility and piezoelectricity, Ceram. Int. 45 (2019) 12663–12671, https://doi.org/10.1016/j.ceramint.2019.03.076.